Osteoarthritis and Cartilage 20 (2012) 916–922

Osteoarthritis and Cartilage

Collagen fibril stiffening in osteoarthritic cartilage of human beings revealed by atomic force microscopy

C.-Y. Wen †[a], C.-B. Wu ‡[a], B. Tang ‡[a], T. Wang †, C.-H. Yan †, W.W. Lu †, H. Pan †, Y. Hu †, K.-Y. Chiu †*

† Department of Orthopaedics and Traumatology, Li Ka Shing Faculty of Medicine, the University of Hong Kong, Hong Kong
‡ Department of Mechanical Engineering, Faculty of Engineering, the University of Hong Kong, Pokfulam, Hong Kong

ARTICLE INFO

Article history:
Received 19 September 2011
Accepted 23 April 2012

Keywords:
Osteoarthritis
Articular cartilage
Collagen fibril
Atomic force microscopy
Nanoindentation

SUMMARY

Objective: This study aimed to characterize the *in-situ* mechanical property and morphology of individual collagen fibril in osteoarthritic cartilage using indentation-type atomic force microscopy (IT-AFM).
Methods: The specimens with intact articular cartilage (AC), mild to severe degenerated cartilage from osteoarthritis (OA) were collected with informed consent from the postmenopausal women who underwent hip or knee arthroplasty. The fresh specimens were cryo-sectioned by layers with 50 μm thick for each from the articular surface to calcified cartilage, and then processed for AFM imaging and nanoindentation test. For each layer, a total of 20 collagen fibrils were randomly selected for testing. AFM tips with the nominal radius less than 10 nm were employed for probing the individual collagen fibril, and the obtained cantilever deflection signal and displacement were recorded for calculating its elastic modulus.
Results: An intact AC exhibited a gradation in elastic modulus of collagen fibrils from articular surface (2.65 ± 0.31 GPa) to the cartilage–bone interface (3.70 ± 0.44 GPa). It was noted in mildly degenerated OA cartilage that the coefficient of variation for mechanical properties of collagen fibers, ranging from 25% to 48%, significantly increased as compared with intact one (12%). The stiffened collagen fibrils occurred at either articular surface (3.11 ± 0.91 GPa) or the cartilage–bone interface (5.64 ± 1.10 GPa), accompanied by loosely organized meshwork with advancement of OA cartilage degeneration. It was echoed by histological findings of OA cartilage, including fibrotic changes of surface region and tidemark irregularities.
Conclusion: The stiffened collagen fibrils in AC occurred with OA onset and progression, not only at articular surface but also the cartilage–bone interface.

Introduction

Osteoarthritis (OA) is a prevalent, debilitating joint disease that leads to disability and poor quality of life in the elderly and induced a heavy social-economic burden[1–3]. The hallmark of OA is articular cartilage (AC) worn out[4]. The process of OA progression was described microscopically: depletion of proteoglycan (PG), breakdown of collagen fibrils network, and mechanical failure of AC, eventually worn out[5]. There are no effective treatments so far to attenuate or cure AC degradation in progressive OA until the damaged joint is reconstructed surgically; therefore, it is necessary to detect OA in very early stage when it remains reversible[6]. However, the exact pathophysiology of OA initiation was ambiguous[6].

With advent of nanobiotechnology, it allows us to tackle OA prior to the occurrence of the microarchitectural damages of AC[7]. For an instance, atomic force microscope (AFM) is now a widely used technique for imaging and mechanical properties testing in biological tissues with its ultra high spatial resolution, fine force sensitivity and versatility under various conditions[8–15]. Stolz *et al.* introduced indentation-type AFM (IT-AFM) for early detection of OA in both animal models and human specimens[15]. They identified a transient increase in the nano stiffness of collagen fibril meshwork at articular surface during OA initiation prior to loss of microarchitectural integrity of AC[15]. Moreover, it was reported in a spontaneous OA model of guinea pigs that the increased collagen fibril cleavage was found prior to PG loss and articular surface fibrillation in osteoarthritic cartilage[16]. The stiff collagen fibril

* Address correspondence and reprint requests to: K.-Y. Chiu, 5/F, Professorial Block, Queen Mary Hospital, Pokfulam, Hong Kong. Tel: 852-2855-4654; Fax: 852-2817-4392.
E-mail address: pkychiu@netvigator.com (K.-Y. Chiu).
[a] The authors equally contributed to this work.

1063-4584/$ – see front matter © 2012 Osteoarthritis Research Society International. Published by Elsevier Ltd. All rights reserved.
doi:10.1016/j.joca.2012.04.018

meshwork in initial stage of OA could be a result of the alterations of individual collagen fibril rather than simply PG loss as Stolz *et al.* once assumed[15]. Therefore, the investigations of the nanomechanical properties of individual collagen fibrils are important for understanding of the onset of OA.

The feasibility of AFM for testing of individual collagen fibril, which was extracted from fibrocartilaginous intervertebral disc tissue, has been demonstrated in previous study[17]. Here, we aimed to investigate the *in-situ* nanomechanical property of individual collagen fibril of AC using AFM and nanoindentation test. To explore the origin of the changes at level of individual collagen fibril with the aging and OA process, we examined the collagen fibrils spatially from articular surface down to the cartilage–bone interface in the intact, or mild to severe degenerated OA cartilage of human beings for comparison.

Methods

Human specimens collection and preparation

All the experimental procedures and protocols were approved by the Institutional Review Board of the authors' institute (Ref Nr: UW 09-368). To explore the origin of individual collagen fibril's changes with aging and OA, the specimens of ACs were purposely obtained from six individual donors with informed consent, include one fresh cadaver knee of healthy young adult women (from Department of Anatomy, Nanfang Medical School, GuangZhou, China), and five aged patients who underwent joint replacement surgery for hip fracture ($n = 1$) or OA ($n = 4$) in authors' institute.

The osteochondral plugs, composing of an AC fragment and subchondral bone, were harvested from each donor at the inferior portion of femoral head (hip) or lateral compartment of tibial plateau (knee) using a biopsy punch with inside diameter of 5 mm. Each osteochondral plug represented the Outerbridge grade 0–3 AC respectively (Table I), which was graded and labeled by an experienced clinician according to the Outerbridge classification system[18]. The specimens were then processed for AFM imaging and nanoindentation. The adjacent osteochondral plugs were also collected for routine histology and scanning electron microscopy (S.E.M.) analysis. The AC fragment of the plugs were embedded using Tissue-Tek and then sectioned by layers with 50 μm in thickness from articular surface down to calcified layer using a cryostatic microtome at −80°C. We selected four representative sections by counting their location in the whole thickness of AC specimens from articular surface down to the cartilage–bone interface, including surface region (5% of thickness), middle region (30% and 70% of thickness) and bottom region (95% of thickness) (Fig. S1). All the sections were immersed in phosphate buffer saline (PBS) and stored in −20°C refrigerators before testing. On the day of testing, the stored AC specimens were thawed and attached onto the glass slip. A standardized procedure, i.e., 30% alcohol washing every 30 min, was applied to partially dehydrate the specimens during AFM imaging and nanoindentation test in order to ensure the degrees of tissue dehydration were comparable among all specimens.

AFM imaging and nanoindentation testing

An AFM machine (Solver Pro47 SPM, NT-MDT Company, Russia) was used in the present study. The AFM imaging and nanoindentation test were conducted using a non-contact AFM tip (NSG20) with the curvature radius of around 10 nm and the relative higher spring constant (28–91 N/m, http://www.ntmdt-tips.com/products/group/non). The AFM imaging procedures were performed under semi-contact mode in order to identify the overlap and gap regions in D-periodic collagen fibrils[19]. AFM nanoindentation tests were performed on randomly selected collagen fibrils, and a total of 20 data points were collected for testing and analysis of each representative layer of AC. It was known that the elastic moduli measured from the overlap region and gap region of collagen fibrils are significantly different[20]. In this study, only the overlap regions of the collagen fibrils were selected for nanoindentation. The use of the non-contact mode minimized the possible specimen surface modification due to tip-sample scratching during the imaging procedures under the semi-contact mode, and also allowed the enough tip-sample penetration during the nanoindentation since the NSG20 tip used has a relative large spring constant (28–91 N/m). High quality AFM images were also taken with a contact AFM tip (CSG10). The AFM nanoindentation process was achieved by controlling the extension/retraction of piezoelectric transducer (PZT) with a computer program written by Nova Powerscript, which is a software designed by the AFM supplier. Firstly, the AFM tip was approached to the sample surface with the set point at 0.1 nA, then the tip retracted for a certain distance with very fast speed to allow AFM tip to depart from the surface of AC samples; after that, the tip moved to the sample surface for 50 nm with the loading rate of 2.11 nm/s, held for 30 s, and finally unloaded with unloading rate 1.35 nm/s (Fig. S2). Here, the holding for 30 s was in an attempt to observe the time-dependent deformation, i.e., the viscoelastic deformation and thermal drift, during the entire indentation procedure. The height and cantilever deflection (DFL) signals were also collected during holding to unloading procedures, to analyze the changes for calculation of the elastic modulus of fibrils. Since the data acquisition rate 50 Hz, a relatively slow unload rate was employed to

Table I
Summary of clinical and laboratory data of healthy and diseased AC

Specimens code	Elastic modulus (GPa) (mean and confidence intervals)					
	Intact AC-adult	Intact AC-aged	OA-0	OA-1	OA-2	OA-3
Number of subject	1	1	1	1	1	1
Age/sex	F/35	F/60	F/59	F/52	F/63	F/70
Clinical diagnosis	Healthy knee	Hip fracture	OA knee	OA knee	OA hip	OA hip
Number of plug for indentation test	1	1	1	1	1	1
Thickness of AC	3.6 mm	4.0 mm	3.5 mm	2.3 mm	1.5 mm	1.15 mm
Outerbridge classification of AC	0	0	0	1	2	3
Number of indentation test performed	20	20	20	20	20	20
Articular surface						
5%	2.65 (2.51–2.80)	2.26 (1.99–2.54)	2.61 (2.22–3.00)	3.11 (2.69–3.54)	3.33 (2.99–3.63)	3.94 (3.40–4.49)
30%	2.67 (2.53–2.82)	2.49 (2.25–2.73)	2.43 (2.17–2.82)	2.43 (2.20–2.66)	3.10 (2.82–3.39)	4.00 (3.61–4.39)
70%	3.14 (2.95–3.34)	2.63 (2.33–2.92)	2.37 (2.09–2.64)	2.80 (2.36–3.25)	3.35 (2.79–3.92)	4.09 (3.50–4.68)
Cartilage–bone interface						
95%	3.70 (3.50–3.91)	3.44 (3.00–3.90)	3.25 (2.52–3.97)	5.64 (5.13–6.16)	4.27 (3.67–4.67)	4.83 (4.22–5.44)

Note: the means and confidence intervals presented were generated from the 20 repeat indentation tests performed on each single specimen.

collect the enough data points for analysis. Actually, the penetration depth of the tip to the sample was less than 50 nm, and also smaller than the thickness of individual collagen fibril, due to the vertical deflection of cantilever.

Before performing the mechanical tests on individual collagen fibrils, the AFM spring constants, e.g., cantilever sensitivity and cantilever-tip constant, were calibrated using our established method and the time-dependent displacement was also measured during the tests simultaneously[21,22]. The assumption of this method was the cylinder shape at the end of the AFM tip. The AFM cantilever deformation and the tip-sample elastic contact were treated as two springs in series (Fig. S3). It was found that, if a loading history containing a sudden load/displacement rate jump is employed, the recorded PZT movement δ and the photodiode signals D before and after the rate jump should follow:

$$\frac{\Delta\dot{\delta}}{\Delta\dot{D}} = A\left(1+\frac{\alpha}{E_r}\right) \quad (1)$$

where α is the tip-cantilever constant, which equals to $k/2a$ (k is the cantilever spring constant and a is the AFM tip radius), A is the cantilever sensitivity, $\Delta\dot{\delta}$ is the displacement rate jump and $\Delta\dot{D}$ is the input rate jump. By performing AFM nanoindentation on two standard materials with known elastic properties, the cantilever sensitivity A and tip-cantilever constant α therefore can be accurately calibrated. The calibrated A and α then can be further used to calculate the elastic modulus of samples desired to be measured if the same experimental setups were employed. Here the two materials used for tip-cantilever constants calibration are a polypropylene (PP) and a fused quartz respectively. The fused quartz is a standard sample with Poisson's ratio 0.16 and elastic modulus 69.5 GPa supplied by Hystrion® company in USA. The elastic modulus of PP sample was measured to be 1.88 GPa using the depth-sensing indentation beforehand. The AFM nanoindentation tests with identical loading schedule as shown in Fig. S2 were performed on the two samples respectively. The spring-tip constants A and α were calibrated based on the recorded DFL and height signals, and are 43.1 nm/nA and 1.08 GPa respectively.

Morphological and compositional evaluation

For the adjacent osteochondral plugs, one was put for ultrastructural and compositional analysis of full-thickness of AC using S.E.M. and energy disperse X-ray spectroscopy (EDX) (Leo 1530 FEG S.E.M.). The other one was decalcified and then processed for routine histological evaluation using Hematoxylin & eosin (H&E) staining.

Results

As shown typical AFM and S.E.M. images (Fig. 1–3), the intact AC was composed of the densely packed collagen fibrils whereas

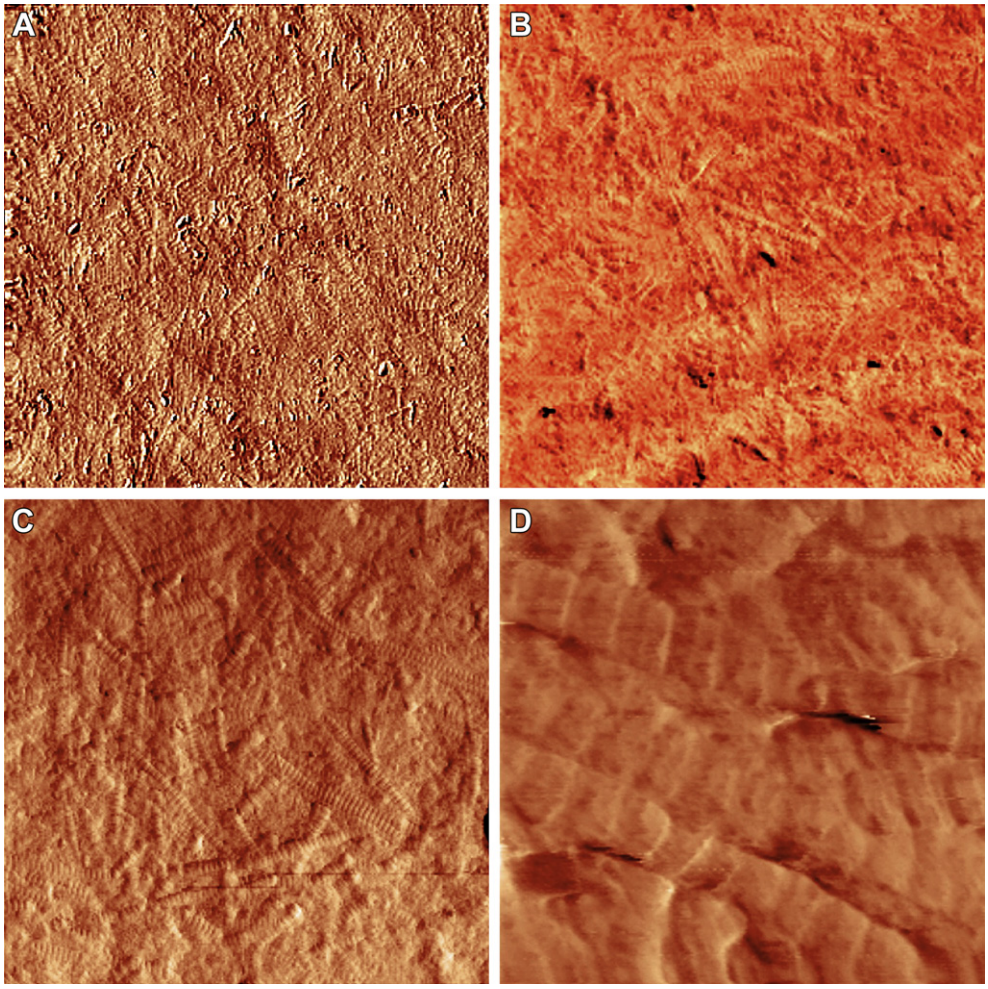

Fig. 1. The representative AFM images showing the individual collagen fibrils of intact AC under low (A–C, 5 × 5 μm) and high magnification (D, 1 × 1 μm). The collagen fibrils from different regions of AC, including the surface (A), middle (B) to the bottom regions (C), were examined respectively. It was much easier under high magnification to identify the D-periodic pattern of individual collagen fibril, e.g., the overlap and gap regions, for the subsequent nanoindentation test (D).

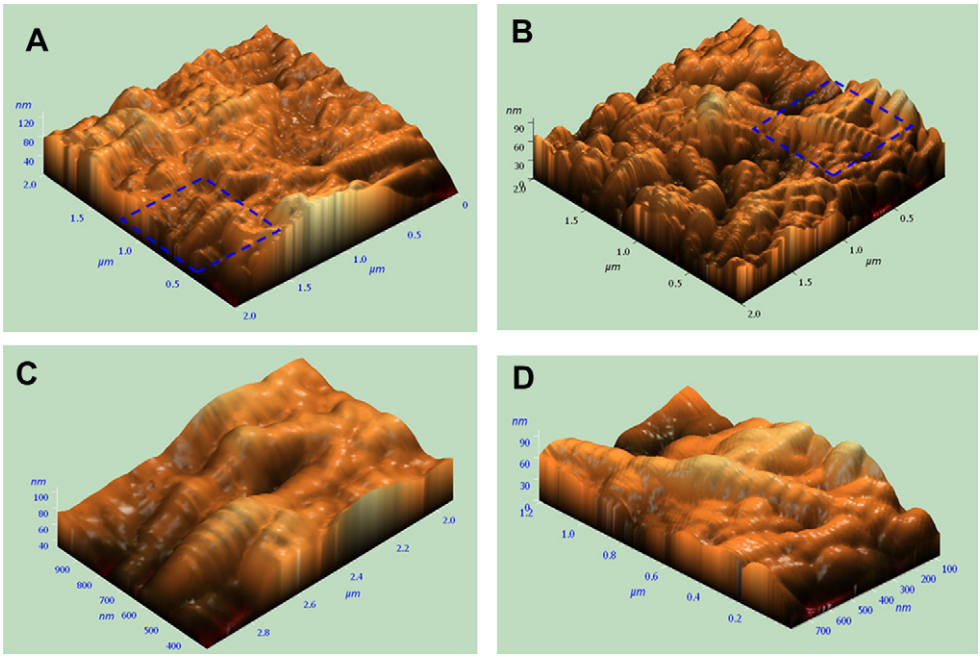

Fig. 2. Three-dimensional AFM images showing *D*-periodic banding pattern of collagen fibrils from healthy (A, C, E) and OA cartilage (B, D, F). High magnification images of C and D were from the regions within dot line in A and B 2 × 2 μm. E and F showed the two-dimensional (2D) AFM images with section measurement on the *D*-periodic banding pattern of collagen fibrils. Line A–A' is the section measured. E and F show the topographic information along the selected sections. *D*-periodic banding patterns of collagen fibrils in intact and OA specimen were 59 nm and 62 nm, respectively.

osteoarthritic cartilage was characterized by poorly organized collagen meshwork. Additionally, there was no significant difference in D-periodic banding pattern between intact and osteoarthritic collagen fibrils (Fig. 2). The nanoindentation was performed on the overlapping region of individual collagen fibril, and the deflection signals dropped significantly during the holding (Fig. 4), which indicated the viscoelastic deformation of collagen fibril. It was revealed under nanoindentation test that the intact AC from healthy adult subject exhibited a gradation in elastic modulus of collagen fibrils from surface region (2.65 ± 0.31 GPa) to bottom region (3.70 ± 0.44 GPa). The intact aged AC also showed the similar trend yet with the relatively larger variation in elastic modulus of individual collagen fibrils, ranging from 19% to 28%. The variation of the modulus of collagen fibrils was larger in OA cartilage, ranging from 26% to 48%. Additionally, the individual collagen fibril of OA cartilage became much stiffer than the intact one, which

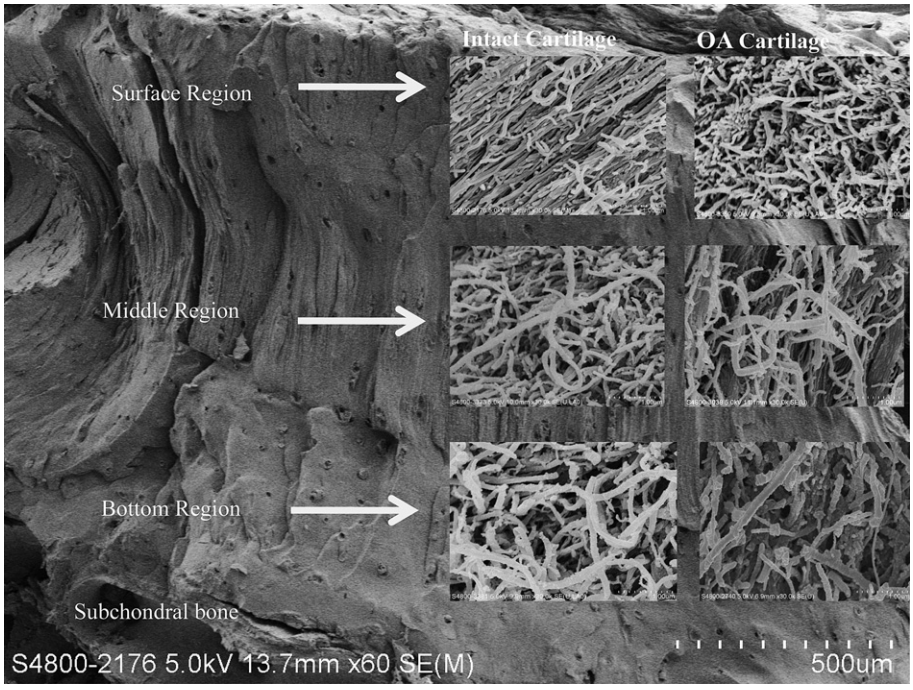

Fig. 3. The representative S.E.M. images showing the organization and diameter of collagen fibrils at different regions of the healthy and osteoarthritic cartilage. The healthy cartilage was composed of compact collagen fibrils whereas the osteoarthritic cartilage was characterized by the loosely organized collagen fibrils.

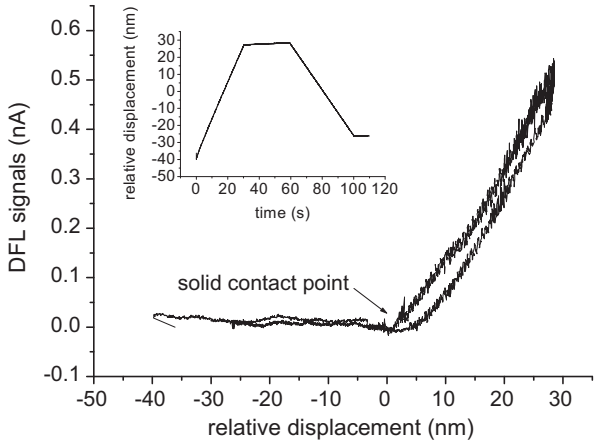

Fig. 4. The representative curves for the displacement and cantilever deflection (DFL) signals obtained in response to the loading schedule (left upper corner), were generated from AFM nanoindentation test performed on collagen fibrils.

was firstly identified at the bottom region (5.64 ± 1.10 GPa) as well as surface region (3.11 ± 0.91 GPa) in early stage of OA (Table 1). With advancement of OA, the collagen fibril stiffening was present throughout the remaining AC along with the breakdown of the collagen meshwork.

As well as loss of collagen meshwork integrity (Fig. 3), the compositional changes in the cartilage–bone unit were examined by S.E.M.–EDX. Results showed the abnormal calcium/phosphate deposition in AC at the bone–cartilage interface (Fig. 4S). These observations were echoed by histopathological findings that fibrotic changes were present at the surface region and disturbance and irregularity of tidemark occurred in between AC and subchondral bone plate (Fig. 5).

Discussions

This study firstly reported the *in-situ* nanomechanical properties of individual collagen fibrils in AC of human beings. For the intact AC from either adult or aged subject, the elastic moduli of

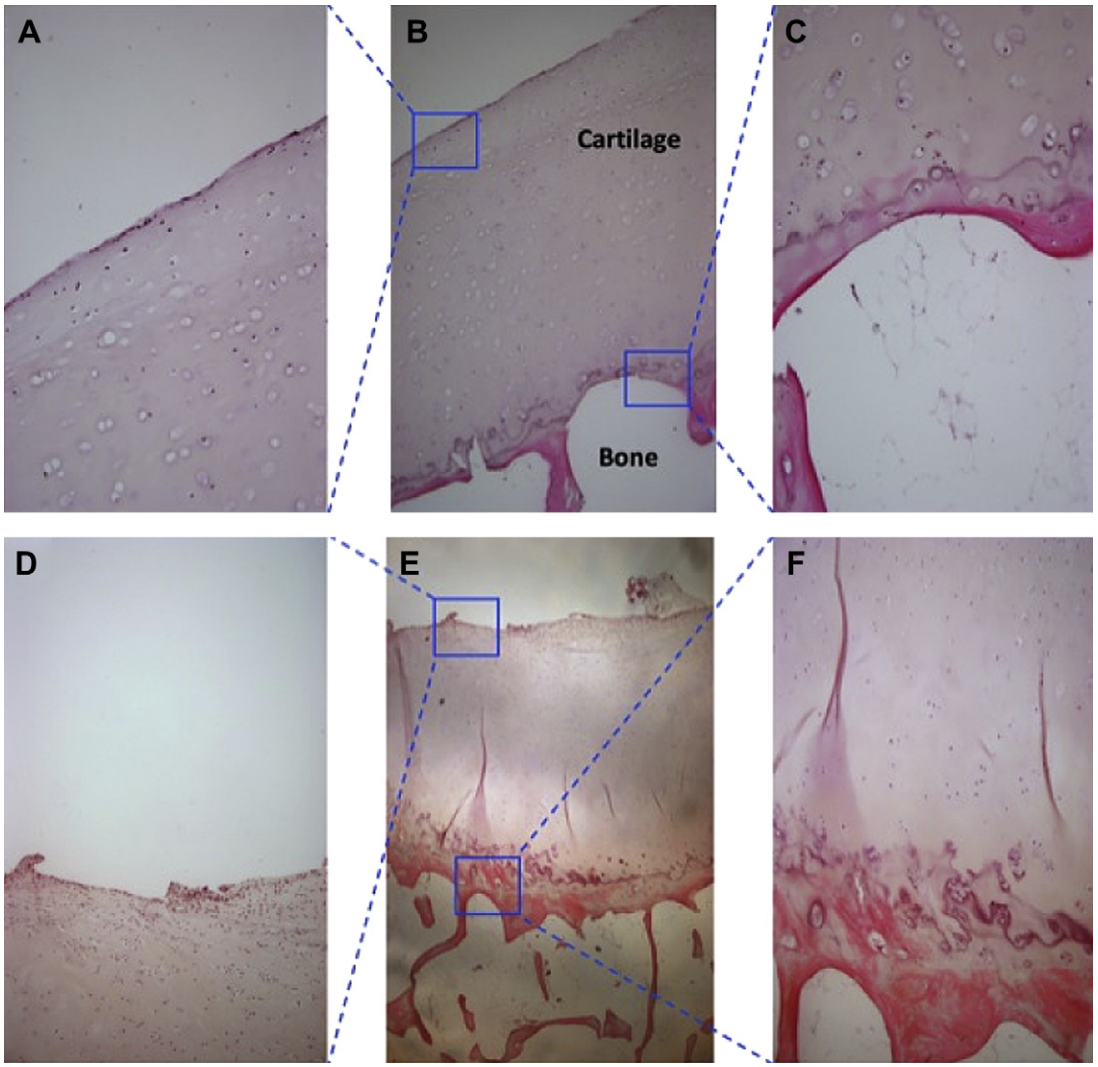

Fig. 5. The representative histological images showed the differences between healthy (A–C) and osteoarthritic AC (D–F). The fibrotic changes at the articular surface (D) and tidemark irregularity (F) at the calcified cartilage were noted in the early stage of OA. (H&E staining; magnification: B and E, 4× and A, C, D and F, 10×).

individual collagen fibrils gradually increased from articular surface to calcified cartilage. Yet the variation for the elastic moduli of individual collagen fibrils of AC slightly increased with the aging process, but dramatically increased during the onset of OA. With progression of OA, the stiffened collagen fibrils occurred at the calcified cartilage as well as articular surface, followed by a significantly drop in the compliance of collagen fibrils of the full-thickness cartilage. It was echoed by the changes in structure and composition of the cartilage–bone unit in OA. The tidemark irregularities together with wrongly deposition of calcium and phosphate were noted at the cartilage–bone interface. It might be associated with the low compliance of collagen fibrils in OA cartilage. The fibrotic changes at articular surface might also explain in part, if not all, the altered nanomechanical properties of collagen fibrils in the surface region of AC.

AC is a highly specialized tissue allowing the low-friction movement, loading bearing and transmission in a diarthrodial joint[23–25]. It is composed of a few cells known as chondrocytes and extracellular matrix, which consists of water and two major molecules components: fibrillar collagen (collagen types II, IX and XI) and PGs. The functional integrity of AC depends on the mechanical properties of the principal matrix components. The collagen fibril meshwork is responsible for tissue integrity and its tensile strength, whilst PG, with their high osmotic pressure, maintains tissue hydration under mechanical stress. It was once detected by IT-AFM that the stiffness of collagen fibril meshwork remarkably increased during the initial stage of OA cartilage in both human beings as well as animal models[15]. Stolz *et al.* interpreted this phenomenon possibly as a result of PG depletion gradually. As reported in this study, the individual collagen fibril stiffening as reported in this study could be also one of possible reasons for increased stiffness of collagen fibrils meshwork in the initial stage of OA. Importantly, the trend of individual collagen fibril stiffening did not change with the breakdown of collagen meshwork with advancement of OA.

It is known now that disruption of collagen fibrils occurred prior to PG loss during the onset of OA[16]. Yet it remains unknown the exact origin of collagen fibrils disruption. Subchondral bone area expansion, could contribute to overlying cartilage damages and the progression of OA[26]. This study demonstrated that collagen fibrils stiffening occurred at the cartilage–bone interface in the mild-degenerated OA cartilage as well as articular surface. Taken together, the disruption of collagen fibril might result from the low compliance of individual collagen fibril under abnormal mechanical loading with subchondral bone changes.

In general, the commercial available AFM tip usually has tip radius smaller than 10 nm, and this enable AFM to be used to probe the nanomechanical properties of tissues with very small size. AFM has been employed to investigate the mechanical of different types of collagen fibrils, including the native collagen fibrils extracted from tissues of the inner dermis of the sea cucumber, collagen fibrils prepared from bovine Achilles tendon, individual type 1 collagen fibrils from rat tail, *etc.* and yield reliable results[20,27–32]. In this study, we firstly explored the *in-situ* mechanical properties of individual type II collagen fibrils.

Technically, the precise determination of experimental constants in IT-AFM evaluation, e.g., cantilever spring constant, tip geometry, cantilever sensitivity, is very crucial for the accuracy of the measurement[9,11,12,21,22]. Moreover, the time-dependent displacements during the tests, e.g., the displacement caused by the viscoelastic deformation and/or thermal fluctuation, will also influence the measurement[21,22,33–37]. In this study, a novel AFM nanoindentation protocol was employed, which can accurate calibrated the cantilever, spring constants in the experiments, as well as deal with the time-dependent displacements, e.g., the viscoelastic deformation, the thermal drift, during the measurement. The individual human collagen fibrils at dehydrated measured in this study is around 2–4 GPa. Nanomechanical properties of individual collagen fibrils type II from ACs of human being were not widely reported so far. However, we can compare with the individual collagen fibrils from different other species: Heim *et al.* measured the Native collagen fibrils extracted from tissues of the inner dermis of the sea cucumber with by radial indentation, and found their elastic modulus is around 1–2 GPa[28]; Collagen fibrils prepared from bovine Achilles tendon at dehydrated state was reported to be 1.9 GPa[27]; individual type I collagen fibrils from rat tail were measured to be 5–15 GPa by Wenger *et al.*[30]. The elastic modulus of collagen fibrils in human ACs measured by us is in the same magnitude. It is therefore believed that the nanomechanical results obtained are rather reliable. It should be admitted that, the mechanical properties of collagen fibrils measured here should be very different from the real properties of collagen fibrils since the samples were dehydrated[27]. However, it should be fine if we only used the obtained results to figure out the differences between intact AC and OA cartilage groups[27].

This is a descriptive laboratory study on *in-situ* nanomechanics of individual collagen fibril in OA cartilage of human beings. Limited to small sample size, no statistical analysis was conducted in this study. The selection of human specimens was arbitrary based on the investigators' experiences. Moreover, the nanoindentation was performed on the partially dehydrated samples rather than fresh ones. These limitations should be known when interpreting the data generated from this study.

In summary, our preliminary findings suggest that IT-AFM is able to detect the low compliance of collagen fibril from AC along with OA initiation and progression. The collagen fibril stiffening combined with biological evidences of collagen fibril disruption might serve as an indicator for early detection of OA.

Author contributions

The authors: Chun-yi Wen, Cheuk-Bun Wu, Bin Tang, Ting Wang, Chun-Hoi Yan, Haobo Pan, William Weijia Lu, Yong Hu, Kwong-yuen Chiu met all the following conditions: (1) substantial contribution to the conception and design (Wen CY; Tang B, Yan CH, Lu WW, Hu Y and Chiu KY), (2) acquisition of data (Wu CB, Tang Bin, Wang T, Pan HB), analysis and interpretation of data, and drafting the article or revising it critically for important intellectual content; also (3) final approval of the version to be published (Wen CY; Tang B, Yan CH, Lu WW).

Conflict of interest

There are no known conflicts of interest associated with this publication and there has been no significant financial support for this work that could have influenced its outcome.

Acknowledgment

The authors acknowledged the General research fund (Project No. HKU 716908E), University Seeding Fund (Project No. HKU10400853) and the Special Equipment Grant (Project No. SEG-HKU06) in support of this study.

Supplementary material

Supplementary material associated with this article can be found, in the online version, at doi:10.1016/j.joca.2012.04.018.

References

1. Anderson AF, Snyder RB, Lipscomb AB. Anterior cruciate ligament reconstruction – a prospective randomized study of three surgical methods. Am J Sports Med 2001;29:272–9.
2. Aune AK, Holm I, Risberg MA, Jensen HK, Steen H. Four-strand hamstring tendon autograft compared with patellar tendon–bone autograft for anterior cruciate ligament reconstruction – a randomized study with two-year follow-up. Am J Sports Med 2001;29:722–8.
3. Herrington L, Wrapson C, Matthews M, Matthews H. Anterior Cruciate Ligament reconstruction, hamstring versus bone-patella tendon–bone grafts: a systematic literature review of outcome from surgery. Knee 2005;12:41–50.
4. Lohmander S. Osteoarthritis year 2010 in review. Osteoarthritis Cartilage 2011;19:337.
5. Martel-Pelletier J, Lajeunesse D, Fahmi H, Tardif G, Pelletier JP. New thoughts on the pathophysiology of osteoarthritis: one more step toward new therapeutic targets. Curr Rheumatol Rep 2006;8:30–6.
6. Pollard TC, Gwilym SE, Carr AJ. The assessment of early osteoarthritis. J Bone Joint Surg Br 2008;90:411–21.
7. Aigner T, Schmitz N, Haag J. Nanomedicine: AFM tackles osteoarthritis. Nat Nanotechnol 2009;4:144–5.
8. Lieber SC, Aubry N, Pain J, Diaz G, Kim SJ, Vatner SF. Aging increases stiffness of cardiac myocytes measured by atomic force microscopy nanoindentation. Am J Physiology Heart Circ Physiol 2004;287:H645–51.
9. Stolz M, Raiteri R, Daniels AU, VanLandingham MR, Baschong W, Aebi U. Dynamic elastic modulus of porcine articular cartilage determined at two different levels of tissue organization by indentation-type atomic force microscopy. Biophys J 2004;86:3269–83.
10. Balooch M, Habelitz S, Kinney JH, Marshall SJ, Marshall GW. Mechanical properties of mineralized collagen fibrils as influenced by demineralization. J Struct Biol 2008;162:404–10.
11. Staple DB, Loparic M, Kreuzer HJ, Kreplak L. Stretching, unfolding, and deforming protein filaments adsorbed at solid–liquid interfaces using the tip of an atomic-force microscope. Phys Rev Lett 2009;102(12):128302.
12. Cai XF, Xing XB, Cai JY, Chen Q, Wu SX, Huang FC. Connection between biomechanics and cytoskeleton structure of lymphocyte and Jurkat cells: an AFM study. Micron 2010;41:257–62.
13. Chan SMT, Neu CP, DuRaine G, Komvopoulos K, Reddi AH. Atomic force microscope investigation of the boundary-lubricant layer in articular cartilage. Osteoarthritis Cartilage 2010;18:956–63.
14. Loparic M, Wirz D, Daniels AU, Raiteri R, VanLandingham MR, Guex G, *et al.* Micro- and nanomechanical analysis of articular cartilage by indentation-type atomic force microscopy: validation with a gel-microfiber composite. Biophys J 2010;98:2731–40.
15. Stolz M, Gottardi R, Raiteri R, Miot S, Martin I, Imer R, *et al.* Early detection of aging cartilage and osteoarthritis in mice and patient samples using atomic force microscopy. Nat Nanotechnol 2009;4:186–92.
16. Huebner JL, Williams JM, Deberg M, Henrotin Y, Kraus VB. Collagen fibril disruption occurs early in primary guinea pig knee osteoarthritis. Osteoarthritis Cartilage 2010;18:397–405.
17. Aladin DM, Cheung KM, Ngan AH, Chan D, Leung VY, Lim CT, *et al.* Nanostructure of collagen fibrils in human nucleus pulposus and its correlation with macroscale tissue mechanics. J Orthop Res 2010;28:497–502.
18. Outerbridge RE, Dunlop JA. The problem of chondromalacia patellae. Clin Orthop Relat Res 1975;110:177–96.
19. Kadler KE, Holmes DF, Trotter JA, Chapman JA. Collagen fibril formation. Biochem J 1996;316(Pt 1):1–11.
20. Minary-Jolandan M, Yu MF. Nanomechanical heterogeneity in the gap and overlap regions of type I collagen fibrils with implications for bone heterogeneity. Biomacromolecules 2009;10:2565–70.
21. Tang B, Ngan AHW, Pethica JB. A method to quantitatively measure the elastic modulus of materials in nanometer scale using atomic force microscopy. Nanotechnology 2008;19(49): 495713.
22. Ngan AHW, Tang B. Response of power-law-viscoelastic and time-dependent materials to rate jumps. J Biomed Mater Res 2009;24:853–62.
23. Minns RJ, Steven FS. The collagen fibril organization in human articular cartilage. J Anat 1977;123:437–57.
24. Broom ND, Poole CA. A functional–morphological study of the tidemark region of articular cartilage maintained in a non-viable physiological condition. J Anat 1982;135:65–82.
25. Clark JM. The organisation of collagen fibrils in the superficial zones of articular cartilage. J Anat 1990;171:117–30.
26. Dore D, Quinn S, Ding C, Winzenberg T, Cicuttini F, Jones G. Subchondral bone and cartilage damage: a prospective study in older adults. Arthritis Rheum 2010;62:1967–73.
27. Grant CA, Brockwell DJ, Radford SE, Thomson NH. Effects of hydration on the mechanical response of individual collagen fibrils. Appl Phys Lett 2008;92:233902.
28. Heim AJ, Matthews WG, Koob TJ. Determination of the elastic modulus of native collagen fibrils via radial indentation. Appl Phys Lett 2006;89:3.
29. Kato K, Bar G, Cantow HJ. The interplay between surface micro-topography and -mechanics of type I collagen fibrils in air and aqueous media: an atomic force microscopy study. Eur Phys J E 2001;6:7–14.
30. Wenger MPE, Bozec L, Horton MA, Mesquida P. Mechanical properties of collagen fibrils. Biophys J 2007;93:1255–63.
31. Yang L, Van der Werf KO, Fitie CFC, Bennink ML, Dijkstra PJ, Feijen J. Mechanical properties of native and cross-linked type I collagen fibrils. Biophys J 2008;94:2204–11.
32. Yang L, van der Werf KO, Koopman B, Subramaniam V, Bennink ML, Dijkstra PJ, *et al.* Micromechanical bending of single collagen fibrils using atomic force microscopy. J Biomed Mater Res A 2007;82A:160–8.
33. Cao GX, Chandra N. Evaluation of biological cell properties using dynamic indentation measurement. Phys Rev E 2010;81.
34. Constantinides G, Kalcioglu ZI, McFarland M, Smith JF, Van Vliet KJ. Probing mechanical properties of fully hydrated gels and biological tissues. J Biomech 2008;41:3285–9.
35. Franke O, Goken M, Hodge AM. The nanoindentation of soft tissue: current and developing approaches. Jom 2008;60:49–53.
36. Lau A, Oyen ML, Kent RW, Murakami D, Torigaki T. Indentation stiffness of aging human costal cartilage. Acta Biomater 2008;4:97–103.
37. Oyen ML, Bushby AJ. Viscoelastic effects in small-scale indentation of biological materials. Int J Surf Sci Eng 2007;1:180–97.